Overview of US Navy SST and Ice Products in the Arctic Seas

Charlie N. Barron[1], Jean-François Cayula[2], Jan M. Dastugue[1], and Jackie C. May[1]
[1] U.S. Naval Research Laboratory, Stennis Space Center, Mississippi, USA
[2] Perspecta, Stennis Space Center, Mississippi, USA

GHRSST XX, 3-7 June 2019, ESA-ESRIN, Frascati (Rome), Italy

Abstract

In prior years, scant attention has been focused on satellite retrieval of sea surface temperature (SST) in the Arctic, as these areas have largely been covered by ice for most of the year. In recent years, thinning ice has exposed increasingly large areas to the infrared satellite sensors, enabling such observations to potentially contribute to global and regional assimilative forecast systems. We focus on VIIRS retrievals, examining these in terms of repeat passes, orbital overlap between consecutive passes, and relative to scattered in situ observations. We also examine the relationship between the SST retrievals and forecasts from the Global Ocean Forecast System (GOFS 3.1) with coupled ocean-ice modeling using the Hybrid Coordinate Ocean Model (HYCOM) and the Community Ice Code (CICE). The ice model provides an ice concentration field that represents the transition from open-ocean through the marginal ice zone to continuous pack ice. These fields inform and are guided by the analysis fields from the Naval ice Center. Choices among various ice edge products or ice concentration levels affect masking choices and confidence in Arctic SST retrievals.

1. SST/Ice Observations and Models

Arctic ice coverage has been in an overall decline in the last few decades (Figure 1), as tracked by the ice extent in September, the month of minimum Arctic ice coverage. This declining ice extent introduces new areas of open water to satellite view and subsequent estimates of sea surface temperature. Prior generations of Navy retrieval software and temperature products assumed that high latitude areas could be safely assumed to be ice covered and or that extrapolation of climatological averages would be sufficient to represent gaps that might sporadically appear. No SST retrievals were processed above 80°N, increased from 70°N five years ago. Reduction in ice coverage has forced these previous assumptions to be discarded, and SST processing at NAVOCEANO has been adopted to use SST from the Navy global coupled ocean + ice forecast system (GOFS 3.1; Metzger et al., 2017) to provide fully global background SST more responsive to changing ice than the legacy NAVOCEANO K10 composite that omitted the high latitudes. This presently affects only the VIIRS processing, as retrievals from geostationary platforms (Himawari and GOES) are limited to lower latitudes.

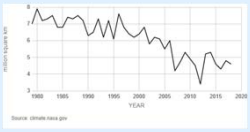

Figure 1: Average September Arctic sea ice extent since 1979, derived from satellite observations. Source is National Snow and Ice Data Center (NSIDC).

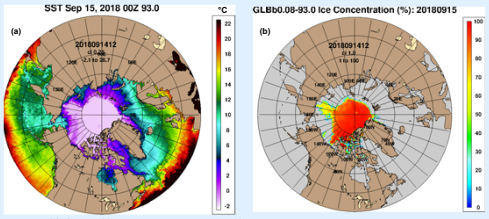

Figure 2: GOFS 3.1 (a) SST and (b) ice concentration on 15 September 2018, near the annual Arctic ice minimum.

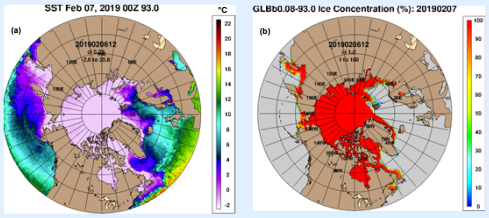

Figure 3: GOFS 3.1 (a) SST and (b) ice concentration on 7 February 2019, near the annual Arctic ice maximum.

GOFS 3.1 SST and ice concentration are shown in cases near minimum (Figures 2a,b) and maximum ice extent (Figures 3a,b). Similar fields from a 3-km resolution Coupled Ocean Atmosphere Prediction System (COAMPS) nested in GOFS 3.1 are shown in Figures 4a,b (Arctic mid-summer) and Figures 5a,b (near Arctic ice minimum). The global model shows the extent of the polar ice cap, while the nested models reveal details in the Greenland Sea. Both models assimilate SST and ice observations via the Navy Coupled Ocean Data Assimilation System (NCODA) including the ice edge from National Ice Center (NIC).

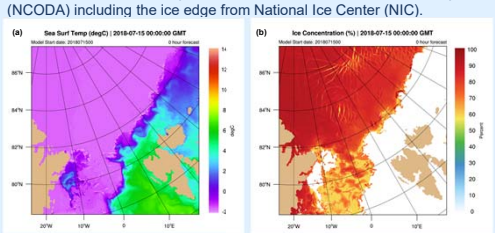

Figure 4: COAMPS (a) SST and (b) ice concentration on 15 July 2018, during Arctic mid-summer.

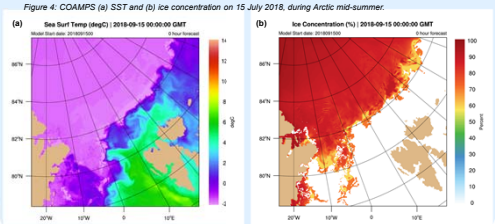

Figure 5: COAMPS (a) SST and (b) ice concentration on 15 September 2018, near the annual Arctic ice minimum.

2. VIIRS SST examples

NRL is testing SST 2.5.x modifications allowing processing of VIIRS SST retrievals at latitudes up to 89°N; prior versions were limited to a 70-80°N maximum. VIIRS SDR data from NOAA-20 for 15 September 2018 and 15 February 2019 are used in producing the L2P SST for the results shown here. Additional data used to show differences and context include the K10 analyzed SST field from NAVOCEANO and the ice concentration and water temperature fields from the operational Global Ocean Forecast system GOFS 5.1. The last two fields are appended to an extended L2P output for the purpose of evaluation. All data are projected in the same azimuthal equidistant projection from the North Pole for evaluation and visualization. All regions are flagged in ice/cloud/contamination detection steps without application of an external ice mask.

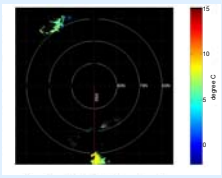

Figure 6: SST field from NOAA-20 VIIRS on 15 February 2019 over the time interval from 11:16 to 11:38 UTC.

Figure 6 shows the SST field. Land, missing or otherwise invalid data (clouds, ice or other contamination) are blacked out. White circles indicate lines of constant latitude, while the red line indicates the International Reference Meridian (IRM).

Figure 7 shows the 10.8μm - 12.0μm brightness temperature difference, while Figure 8 plots the reflectance. Only land and missing data are blacked out in these figures. In this selection of data near noon UTC on a winter day in the Northern hemisphere, the sun is in the oriented toward the bottom of the plot and the higher latitudes are in continual darkness. Thus the brightness temperature values near the upper left corner are retrieved under conditions of darkness that correspond to zero reflectance as there is nothing to reflect. A few retrievals in the 70N°-80N° range are identified as representing valid sea surface temperatures through gaps in the prevailing ice and clouds.

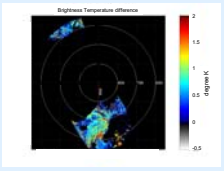

Figure 7: 10.8μm - 12.0μm brightness temperature difference from NOAA-20 VIIRS on 15 February 2019 over the time interval from 11:16 to 11:38 UTC.

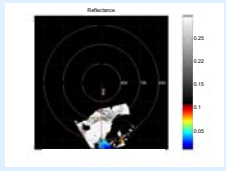

Figure 8: Reflectance field from NOAA-20 VIIRS on 15 February 2019 over the time interval from 11:16 to 11:38 UTC.

Figure 9 shows the NAVOCEANO K10 analyzed SST (composite of latest retrievals) and Figure 10 shows the difference between Figures 6 and 9: NOAA-20 VIIRS SST – K10. Only land and missing data are blacked out.

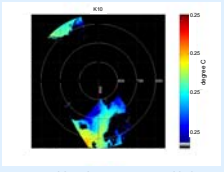

Figure 9: NAVOCEANO K10 daily composite SST field on 15 February 2019.

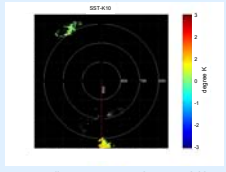

Figure 10: Difference between the NOAA 20 VIIRS SST retrievals from Figure 6 and the K10 analyzed SST field (Figure 9) (VIIRS – K10). These show warming in day temperatures, neutral in night temperatures relative to K10.

Figures 11 and 12 display GOFS 3.1 SST (uppermost water temperature) and ice concentration respectively. Those are appended to an extended L2P output for reference and further evaluation. Unlike the K10 SST field where ice areas are masked based on an overlay from the NIC, the GOFS water temperature field can be used in conjunction with ice concentration field from the same model to flag ice regions where the model values indicate liquid water temperatures under ice.

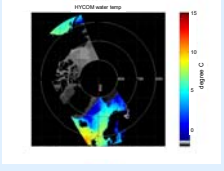

Figure 11: GOFS 3.1 SST field on 15 February 2019.

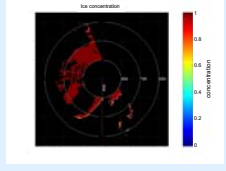

Figure 12: GOFS 3.1 ice concentration field on 15 February 2019.

3. SST Overlap Evaluation

Consecutive orbits at high latitude have large overlaps with the result that locations at high latitudes are more frequently visited than those at low latitude which in turn reduces potential gaps in composite SST fields. Figure 13 shows the composite SST field built from all orbits from 15 February 2019 using the most recent valid data at each location. Figure 14 shows the largest differences between consecutive orbits over this day. The increased overlap between orbits at high latitudes allows for a higher number of comparison points between consecutive orbits, offering a measure of the representativeness on the SST retrievals.

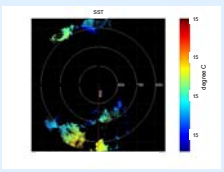

Figure 13: Composite SST field built from all orbits sampled on 15 February 2019.

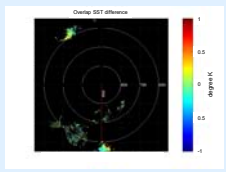

Figure 14: Composite orbital overlap SST difference on 15 February 2019. The largest differences between consecutive orbits are displayed.

4. Northern Hemisphere Ice Minimum

Previous-generation NAVOCEANO SST processing employs a mask based on externally-derived ice coverage to exclude areas with insufficient open water for reliable satellite estimates of SST. However a goal is to rely on direct satellite measurement, such as brightness temperatures, to flag areas that are invalid for SST retrievals, including areas with excessive ice or cloud contamination. Figure 15 shows the daytime composite SST from NPP VIIRS on 15 September 2018, with the corresponding daytime reflectance composite in Figure 16. For display purpose, areas with reflectance values exceeding 0.1 are shaded in grays and white, approximately indicating location where cloud and/or ice are expected to degrade SST.

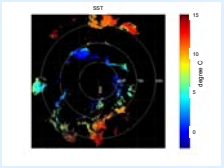

Figure 15: Daytime composite SST from NPP VIIRS on 15 September 2018.

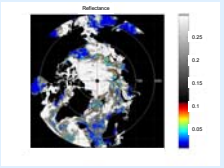

Figure 16: Daytime composite NPP VIIRS reflectance on 15 September 2018.

During daytime, subject to the satellite and solar angles, high values of the reflectance are the best indicator of ice or cloud contamination. At night when the reflectance is too low, the more effective test compares the 3.7μm brightness temperature (BT) from a proxy 3.7μm BT estimated from the 10.8μm and 12.0μm channels: |3.7μm BT – $f_{3.7}$(10.8μm BT, 12.0μm BT)|. The retrievals also pass through a supplemental test based on the difference of the BT from the 10.8μm and 12.0μm channels. The BT difference test (Figure 17) sets upper and lower thresholds as a function of estimated SST. This test does not seem effective in identifying ice contamination; its application, day and night, targets other contamination sources.

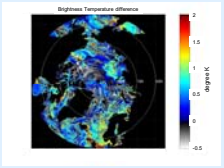

Figure 17: Composite NPP VIIRS daytime BT difference, 15 September 2018

The composite SST and reflectance indicator of potential ice/cloud contamination can be compared with the prediction of the global ocean forecast models for the same day. The composite uppermost water temperature and ice concentration from GOFS 3.1 are shown in Figures 18 and 19, respectively. Note that the GOFS 3.1 water temperatures include values at locations under ice; these are shaded gray.

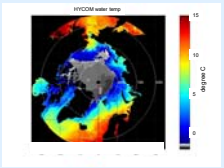

Figure 18: GOFS 3.1 SST field on 15 September 2018.

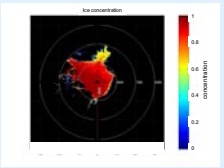

Figure 19: GOFS 3.1 ice concentration field on 15 September 2018.

The composite field of SST differences calculated across overlapping orbits on this day are depicted in Figure 20. At high latitudes, retrievals from polar orbits overlap more frequently, making this a likely candidate for more reliable testing and validation of SST in the Arctic. The tests above rely solely on the measurements by the satellite sensors without introducing external fields or analyses. This is the preferred approach in the latest SST processing software. Other tests may be based on screening out retrievals exceeding a threshold difference from a prior analysis or composite SST field. An example of input for such a test is included in Figure 21, showing a composite of maximum differences between SST retrievals relative to the prior K10 SST analysis.

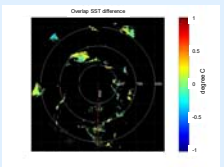

Figure 20: Composite orbital overlap SST difference on 15 September 2018.

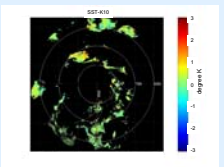

Figure 21: Composite SST retrieval – K10 difference on 15 September 2018.

5. Discussion

Developments in SST processing underway at NRL and NAVOCEANO are leading to more comprehensive capabilities to derive SST retrievals at high latitudes while avoiding negative effects from contamination associated with ice, clouds, or other factors. Procedures are adapting to the challenges and opportunities unique to these conditions. Work on leveraging ice analyses and forecasts continue, seeking to quantify changes from open water into the marginal ice zone. As we continue to identify more reliable approaches to define flagging methods solely dependent on satellite observations, external models and ice analysis products offer supplemental information to identify the effects of ice and other contaminants on reliability of Arctic retrieval and identify false negative or false positive flagging of SST retrievals. Work will expand from VIIRS to Metop-C as a source of satellite observations, adding potentially additional cross-over comparisons to identify reliability and temporal variability of retrievals as a function of proximity to various concentration contours within the marginal ice zone.

Acknowledgements

This research was made possible in part by the Office of Naval Research through their support of the Multi-sensor Improved Sea Surface Temperature: continuing the GHRSST partnership and improving Arctic data (MISST-Arctic) project.